




## Tetrakis(thione)platinum(II) complexes: synthesis, spectroscopic characterization, crystal structures, and in vitro cytotoxicity

A. Zainelabdeen A. Mustafa, M. Monim-ul-Mehboob, M. Y. Jomaa, M. Altaf, M. Fettouhi, A. A. Isab, M. I. M. Wazeer, H. Stoeckli-Evans, G. Bhatia & V. Dhuna


To cite this article: A. Zainelabdeen A. Mustafa, M. Monim-ul-Mehboob, M. Y. Jomaa, M. Altaf, M. Fettouhi, A. A. Isab, M. I. M. Wazeer, H. Stoeckli-Evans, G. Bhatia & V. Dhuna (2015) Tetrakis(thione)platinum(II) complexes: synthesis, spectroscopic characterization, crystal structures, and in vitro cytotoxicity, *Journal of Coordination Chemistry*, 68:19, 3511-3524, DOI: [10.1080/00958972.2015.1072175](https://doi.org/10.1080/00958972.2015.1072175)



To link to this article: <http://dx.doi.org/10.1080/00958972.2015.1072175>

 View supplementary material 

 Accepted author version posted online: 30 Jul 2015.  
Published online: 24 Aug 2015.

 Submit your article to this journal 

 Article views: 92

 View related articles 

 View Crossmark data 

## Tetrakis(thione)platinum(II) complexes: synthesis, spectroscopic characterization, crystal structures, and *in vitro* cytotoxicity

A. ZAINELABDEEN A. MUSTAFA<sup>†</sup>, M. MONIM-UL-MEHBOOB<sup>†</sup>, M. Y. JOMAA<sup>†</sup>,  
M. ALTAF<sup>†,1</sup>, M. FETTOUHI<sup>†</sup>, A. A. ISAB<sup>\*†</sup>, M. I. M. WAZEER<sup>†</sup>,  
H. STOECKLI-EVANS<sup>‡</sup>, G. BHATIA<sup>§</sup> and V. DHUNA<sup>\*¶</sup>

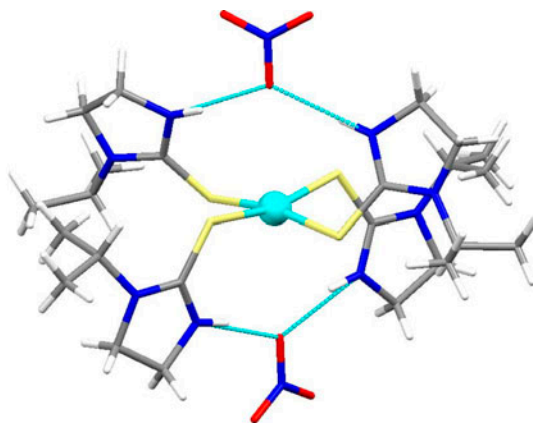
<sup>†</sup>Department of Chemistry, King Fahd University of Petroleum and Minerals, Dhahran, Saudi Arabia

<sup>‡</sup>Institute of Physics, University of Neuchâtel, Neuchâtel, Switzerland

<sup>§</sup>Department of Molecular Biology and Biochemistry, Guru Nanak Dev University, Amritsar, India

<sup>¶</sup>Department of Biotechnology, DAV College, Amritsar, India

(Received 6 February 2015; accepted 22 June 2015)



A new series of platinum(II) complexes based on thione ligands with general formula  $[Pt(\text{thione})_4]X_2$  ( $X^- = Cl^-, NO_3^-$ ) has been synthesized and characterized using CHNS elemental analysis, infrared,  $^1H$  and  $^{13}C$  solution-state NMR as well as  $^{13}C$  and  $^{15}N$  solid-state NMR spectroscopy, and X-ray crystallography. The spectroscopic methods confirm the coordination of Pt(II) with thiocarbonyl groups via sulfur of the thione ligands. The X-ray structures showed a distorted square planar geometry for **1**,  $[Pt(\text{Melmt})_4]Cl_2$  (Melmt = N-Methylimidazolidine-2-thione) while the hydrogen bonding interactions in **7**,  $[Pt(iPrImt)_4](NO_3)_2 \cdot 0.6(H_2O)$  induce a bent see-saw distortion relative to the ideal square planar geometry. The *in vitro* cytotoxicity studies showed that **2**,  $[Pt(EtImt)_4]Cl_2$  is generally the most effective, a two-fold better cytotoxic agent than cisplatin and carboplatin against MCF7 (human breast cancer).

**Keywords:** Pt(II) thione complexes; N-Alkylimidazolidine-2-thione; N-Ethyl-1,3-diazinane-2-thione; 1,3-Diazipane-2-thione; NMR; *In vitro* cytotoxicity

\*Corresponding authors. Email: [aaisab@kfupm.edu.sa](mailto:aaisab@kfupm.edu.sa) (A.A. Isab); [vikramdhuna@gmail.com](mailto:vikramdhuna@gmail.com) (V. Dhuna)

<sup>1</sup>Present address: Center of Excellence in Nanotechnology, King Fahd University of Petroleum and Minerals, Dhahran, Saudi Arabia.

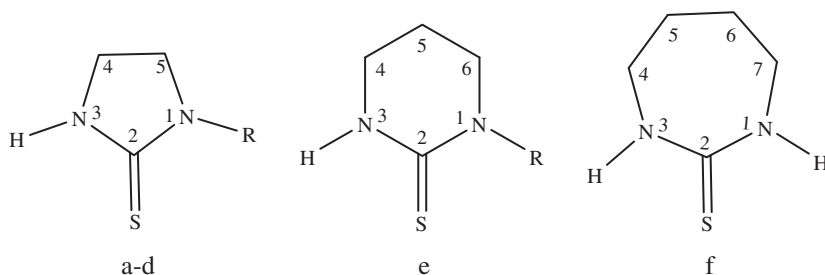
## 1. Introduction

Since the discovery of the platinum(II)-based drug cisplatin [1], its clinical use has been reduced by its severe side effects such as nephrotoxicity [2] and gastrointestinal effects [3], and also by the resistance of cancer cells to the drug. As a result, several alternative platinum complexes have been synthesized to overcome these side effects. Platinum(II) complexes that have the classical structure  $cis-[PtX_2(NHR_2)_2]$ , in which X = leaving group and R = organic fragment, bind to DNA through 1,2-intrastrand cross-links, between N7 of two adjacent guanines (G) with platinum(II) [4–6].

The search for a new generation of platinum(II) complexes, which are able to broaden the biological activity spectrum and eliminate the multifactorial drug resistance, resulted in the synthesis of platinum(II) complexes containing biologically active ligands. These complexes are supposed to interact with DNA through a mechanism different from that of cisplatin. Studies found that cisplatin-like drugs could introduce nephrotoxicity due to their reaction with sulfur-containing amino acids of the proteins: cysteine and methionine [6]. Platinum(II) complexes with sulfur-containing ligands, like dimethyl sulfoxide (DMSO), dimethyl sulfide, xanthate, and thiosemicarbazones [7–9], have shown high efficacy against some human cancer cell lines.

Thiourea and its derivatives as sulfur-containing ligands are expected to give better results if they coordinate with platinum(II) center. They have been used as antifungal agents [10], rescue agents against nephritic side effects during cisplatin administration, and as inhibitors of HIV-1 and HIV-2 reverse transcriptases [11]. Platinum(II) complexes with thiourea ligands demonstrated that they can bind to DNA in a different mechanism to that of cisplatin and showed an excellent cytotoxicity against ovarian and leukemia cancer cell lines [12, 13].

Such success of thiourea and its derivatives in cancer treatment encouraged us to synthesize new platinum(II) complexes with thiourea derivatives and characterize those using different analytical and spectroscopic techniques. Along this line, tetrakis(1–3-diazinane-2-thione)platinum(II) chloride monohydrate was recently synthesized and evaluated *in vitro* for cytotoxic activity against a panel of cancer cell lines [14]. In continuation of this research, we report herein the synthesis, spectroscopic, and X-ray structural characterization and *in vitro* cytotoxicity of a new series of platinum(II) complexes (1–7) based on the structurally different thione ligands, shown in scheme 1.



Scheme 1. Structures of different thione ligands. (a) R = CH<sub>3</sub>; N-methylimidazolidine-2-thione (MeImt), (b) R = C<sub>2</sub>H<sub>5</sub>; N-ethylimidazolidine-2-thione (EtImt), (c) R = C<sub>3</sub>H<sub>7</sub>; N-propylimidazolidine-2-thione (PrImt), (d) R = *i*-C<sub>3</sub>H<sub>7</sub>; N(*i*-propyl)imidazolidine-2-thione (*i*-PrImt), (e) R = C<sub>2</sub>H<sub>5</sub>; N-ethyl-1,3-diazinane-2-thione (EtDiaz) and (f) 1,3-Diazepane-2-thione (Diap).

## 2. Experimental

### 2.1. Chemicals and reagents

Potassium tetrachloridoplatinate(II),  $K_2PtCl_4$ , was purchased from Strem Chemicals, Inc. Carbon disulfide ( $CS_2$ ) and diamines *i.e.* N-methyl-1,2-diaminoethane, N-ethyl-1,2-diaminoethane, N-propyl-1,2-diaminoethane, and N-isopropyl-1,2-diaminoethane, N-ethyl-1,3-diaminopropane, 1,4-diaminobutane, were obtained from Sigma Aldrich. Dulbecco's modified eagle medium (DMEM), (3-(4,5-dimethylthiazol-2-yl)-2,5-diphenyltetrazolium bromide) (MTT), DMSO and deuterated solvents were also obtained from Sigma Aldrich Chemical Co. All other solvents were obtained from Fluka Chemical Co., and used without purification.

### 2.2. Synthesis of the compounds

**2.2.1. Thione ligands.** The thione ligands were synthesized using a procedure given in the literature [15, 16] by the reaction of carbon disulfide ( $CS_2$ ) with diamines in diethyl ether. The resultant mixture was then refluxed at 100–110 °C for 2–3 h. The clear yellow product was recrystallized from methanol.

**2.2.2. General procedure for the synthesis of  $[Pt(\text{thione})_4]Cl_2$  complexes 1–6.**  $K_2PtCl_4$  (0.500 mmol) in 3.0 mL of water and thione (2.00 mmol) in 25.0 mL hot water were mixed and refluxed for 4 h. A yellow solution was finally obtained. It was filtered while hot. The solvent was evaporated. Quality yellow-orange crystals of **1** suitable for X-ray diffraction were obtained by slow evaporation of the solvent. The CHNS data, melting/decomposition points, and % yield of the synthesized complexes are presented below:

Complex **1**:  $[Pt(\text{MeImt})_4]Cl_2 \cdot 2H_2O$ : C 24.91 (25.06), H 4.61 (4.73), N 14.51 (14.62), S 16.36 (16.73) decomposition point 262 °C, and yield 58.9%; Complex **2**:  $[Pt(\text{EtImt})_4]Cl_2$ : C 30.56 (30.53), H 5.01 (5.12), N 14.46 (14.24), S 16.47 (16.30); decomposition point 225 °C and yield 64.3%; Complex **3**:  $[Pt(\text{PrImt})_4]Cl_2$ : C 33.98 (34.20), H 5.40 (5.47), N 13.35 (13.30), S 12.34 (12.22); decomposition point 106 °C and yield 89.3%; Complex **4**:  $[Pt(i\text{-PrImt})_4]Cl_2$ : C 34.22 (34.20), H 5.33 (5.47), N 13.21 (13.30), S 12.27 (12.22); melting point 145 °C and yield 92.5%; Complex **5**:  $[Pt(\text{EtDiaz})_4]Cl_2$ : C 33.80 (34.19), H 5.82 (5.74), N 13.10 (13.29), S 12.24 (12.22); melting point 113 °C and yield 52.5%; Complex **6**:  $[Pt(\text{Diap})_4]Cl_2$ : C 30.27 (30.53), H 5.22 (5.12), N 14.13 (14.24), S 16.12 (16.30); decomposition 285 °C and yield 35.3%.

**2.2.3. Synthesis of  $[Pt(i\text{PrImt})_4](NO_3)_2 \cdot 0.6(H_2O)$  (**7**).** 168.8 mg (1.000 mmol) of  $AgNO_3$  was added to solution containing 150.06 mg (0.500 mmol) of  $K_2PtCl_4$  in 10.0 mL water and stirred for 24 h in the dark at room temperature, then filtered. 288.2 mg (2.000 mmol) of N-*i*-Propyl-Imt dissolved in 10.0 mL methanol was added to the filtrate. The brown solution was filtered after stirring for 3 h and the filtrate was kept at room temperature for evaporation to afford X-ray quality crystals. Complex **7**:  $[Pt(i\text{PrImt})_4](NO_3)_2 \cdot 0.6(H_2O)$ : C 31.04 (31.78), H 5.18 (5.48), N 15.57 (15.44), S 13.99 (14.14); melting point 119 °C and yield 42.9%.

### 2.3. Stability and solubility of 1–7

Complexes **1**, **5**, and **6** were dissolved in DMSO- $d_6$  and their  $^1\text{H}$  NMR spectra were measured. The extent of decomposition over time was determined by comparing the NMR spectra collected after 1, 6, 12, 24, 48, and 72 h. No significant change in the chemical shifts and the splitting patterns of **1** and **2** was observed in their time dependent  $^1\text{H}$  NMR spectra. Complex **1** was moderately soluble in  $\text{CDCl}_3$  but completely soluble in DMSO and DMF. Complexes **2–7** were completely soluble in polar organic solvents *i.e.*  $\text{CDCl}_3$ , DMSO, and DMF.

### 2.4. Spectroscopic and other characterization methods

The solid-state FT-IR spectra of thione ligands and their corresponding tetrakis(thione) platinum(II) chloride or nitrate complexes (**1–7**) were recorded on a Nicolet 6700 FTIR spectrometer using KBr pellets from 4000 to 400  $\text{cm}^{-1}$ .  $^1\text{H}$  NMR spectra were obtained on a Jeol JNM-LA 500 NMR spectrometer operating at a frequency of 500.00 MHz.  $^{13}\text{C}$  NMR spectra were obtained at the frequency of 125.65 MHz with  $^1\text{H}$  broadband decoupling at 298 K. The spectral conditions were: 32 k data points, 0.967 s acquisition time, 1.00 or 30.00 s pulse delay, and  $45^\circ$  pulse angle. Elemental analyses for the platinum(II) thione complexes were performed on a Perkin Elmer 2400 Series II CHNS/O Analyzer.

### 2.5. X-ray diffraction analysis

For **1**, the X-ray diffraction data were recorded on a Bruker-Axs Smart Apex system equipped with graphite monochromated  $\text{MoK}\alpha$  radiation ( $\lambda = 0.71073 \text{ \AA}$ ). The data were collected using SMART [17]. The data integration was performed using SAINT [18]. An empirical absorption correction was carried out using SADABS [19]. The structure was solved with direct methods and refined by full-matrix least-squares based on  $F^2$  using the structure determination package SHELXTL [20] based on SHELX 97 [21]. Graphics were generated using ORTEP-3 [22] and Mercury [23]. With the help of a riding model, H-atoms other than those of the water molecules were included at calculated positions. Nitrogens belonging to NH groups were assumed to have  $\text{sp}^2$  hybridization. The hydrogens of the water molecules could not be located.

For **7**, the intensity data were collected at 173 K ( $-100^\circ\text{C}$ ) on a Stoe Mark II-Image Plate Diffraction System [24] equipped with a two-circle goniometer and using  $\text{MoK}\alpha$  graphite monochromated radiation ( $\lambda = 0.71073 \text{ \AA}$ ). The structure was solved by direct methods with SHELXS-2014 [21]. The refinement and all further calculations were carried out with SHELXL-2014 [21]. The hydrogens were either located from Fourier difference maps and freely refined or included in calculated positions and treated as riding using SHELXL default parameters. The non-H atoms were refined anisotropically using weighted full-matrix least-squares on  $F^2$ . Empirical or multiscan absorption corrections were applied using the MULSCANABS routines in PLATON [25]. A summary of crystal data and refinement details for **1** and **7** are given in table 1.

Table 1. Crystal and structure refinement data for **1** and **7**.

Parameter	<b>1</b>	<b>7</b>
CCDC deposit no.	902,467	1,008,031
Empirical formula	C <sub>16</sub> H <sub>36</sub> Cl <sub>2</sub> N <sub>8</sub> O <sub>2</sub> PtS <sub>4</sub>	C <sub>24</sub> H <sub>49.20</sub> N <sub>10</sub> O <sub>6.60</sub> PtS <sub>4</sub>
Formula weight	766.76	906.86
Temperature (K)	296(2)	173(2)
Wavelength (Å)	0.71073	0.71073
Crystal system	Triclinic	Tetragonal
Space group	<i>P</i> -1	<i>P</i> 4 <sub>3</sub> 2 <sub>1</sub> 2
Unit cell dimensions		
<i>a</i> (Å)	9.011(2)	11.608(3)
<i>b</i> (Å)	9.424(2)	11.608(3)
<i>c</i> (Å)	9.627(2)	27.182(1)
$\alpha$ (°)	92.275(4)	90
$\beta$ (°)	99.333(4)	90
$\gamma$ (°)	116.185(3)	90
Volume (Å <sup>3</sup> )	718.2(3)	3662.7(2)
<i>Z</i>	1	4
Calcd density (g cm <sup>-3</sup> )	1.773	1.645
Absorp. coefficient (mm <sup>-1</sup> )	5.39	4.11
<i>F</i> (0 0 0)	380	1832
Crystal size (mm)	0.27 × 0.22 × 0.15	0.45 × 0.35 × 0.20
$\theta$ range (°)	2.16–28.37	1.9–26.1
Limiting indices	–12 ≤ <i>h</i> ≤ 11 –12 ≤ <i>k</i> ≤ 12 –12 ≤ <i>l</i> ≤ 12	–14 ≤ <i>h</i> ≤ 14 –14 ≤ <i>k</i> ≤ 13 –32 ≤ <i>l</i> ≤ 33
Max and min transmission	<i>T</i> <sub>min</sub> = 0.3239, <i>T</i> <sub>max</sub> = 0.4986	<i>T</i> <sub>min</sub> = 0.7681, <i>T</i> <sub>max</sub> = 1.0000
Data/restraints/parameters	3552/0/153	3457/5/230
Goodness-of-fit on <i>F</i> <sup>2</sup>	1.041	0.875
Final <i>R</i> indices [ <i>I</i> > 2σ( <i>I</i> )]	<i>R</i> <sub>1</sub> = 0.0255, <i>wR</i> <sub>2</sub> = 0.0543	<i>R</i> <sub>1</sub> = 0.0153, <i>wR</i> <sub>2</sub> = 0.0265
<i>R</i> indices (all data)	<i>R</i> <sub>1</sub> = 0.0193, <i>wR</i> <sub>2</sub> = 0.0545	<i>R</i> <sub>1</sub> = 0.0259, <i>wR</i> <sub>2</sub> = 0.0269
Largest diff. peak and hole (eÅ <sup>-3</sup> )	1.310 and –0.842	0.34 and –0.75

## 2.6. MMT assay for *in vitro* cytotoxic studies of [Pt(thione)<sub>4</sub>]Cl<sub>2</sub> compounds against a panel of cancer cell lines

In the present study, [Pt(thione)<sub>4</sub>]Cl<sub>2</sub> complexes **1–7** were tested for their *in vitro* cytotoxicity against MCF7 (human breast cancer), HCT15 (human colon adenocarcinoma), HeLa (human cervical cancer), and A549 (human lung carcinoma) cell lines as reported [26]. The cells were seeded at  $3 \times 10^3$  cells/well in 100  $\mu$ L DMEM containing 10% fetal bovine serum (FBS) in a 96-well tissue culture plate and incubated for 72 h at 37 °C, 5% CO<sub>2</sub> in air, and 90% relative humidity in a CO<sub>2</sub> incubator. After incubation, 100  $\mu$ L of 50, 25, 12.5, and 6.25  $\mu$ M solutions of platinum(II) complexes, prepared in DMEM, were added to the cells and the cultures were incubated for 24 h. The medium of wells was discarded and 100  $\mu$ L DMEM containing MTT (0.5 mg mL<sup>-1</sup>) was added to the wells and incubated in a CO<sub>2</sub> incubator at 37 °C in the dark for 4 h. After incubation, a purple formazan produced in the cells appeared as dark crystals in the bottom of the wells. The culture medium was discarded from each well carefully to prevent disruption of the monolayer and 100  $\mu$ L of DMSO was added in each well. The solution in the wells was thoroughly mixed to dissolve the formazan crystals which produce a purple solution. The absorbance of the 96 well-plates was taken at 570 nm with a Labsystems Multiskan EX ELISA reader against a reagent blank. The experimental results are presented as micro-mole concentration of 50% cell growth inhibition (IC<sub>50</sub>) of each drug. The MTT assay was performed in three independent experiments, each in triplicate.

### 3. Results and discussion

#### 3.1. FT-IR spectroscopic characterization

The most important selected FT-IR frequencies are quoted in table 2. As mentioned by many authors, the assignment of the thioamide absorptions of free thiones and their related compounds is not straight forward, due to strong coupling between thiocarbonyl absorption and various bond absorptions in the fingerprint region of the FTIR spectrum [27–30]. Nevertheless, a strong and broad band at 1400–1600  $\text{cm}^{-1}$  appears for all the thione ligands and their related complexes. Based on the data of previous literature, this band must be due to (N–H) deformation and (N–C–N) antisymmetric stretching. This band is often split and significantly shifted to higher frequency upon complexation; this is an indication of increase in the double bond character of the C–N bond due to coordination with sulfur [29–31]. The band observed at 3220–3300  $\text{cm}^{-1}$  for most of the thione ligands and their related complexes is directly assigned for N–H stretching vibrations [27–30, 32]. This band shifts to higher frequencies for most of the platinum(II) complexes due to increase in double bond character, which also supports the idea of coordination with the sulfur of thiocarbonyl in the thione form. The assignment of thiocarbonyl frequencies is the most difficult part in the FTIR spectra because it strongly couples with other bonds within the molecule and gives many bands in the fingerprint region. Many absorption bands in the FTIR spectrum of the free thiones, for instance MeImt: 1236, 1111, 957, 670, 637, 612, and 516  $\text{cm}^{-1}$ , have shifted to lower wave number with not more than 21  $\text{cm}^{-1}$  in its related corresponding complex, and could be assigned to thiocarbonyl frequencies [28]. The same pattern of this shift has been noticed for most of the platinum(II) complexes which indicate the presence of the Pt–S bond. Finally, it seems appropriate to obtain more definitive evidence of the coordination site through NMR spectroscopy and X-ray crystallography, discussed in the forthcoming parts.

#### 3.2. Solution and solid-state NMR characterization

The  $^1\text{H}$  NMR chemical shifts of the free thione ligands and their corresponding complexes were studied in 50 : 50 v/v ratio of a mixture of  $\text{CDCl}_3$  and DMSO solvents, except **5** which was studied in  $\text{CDCl}_3$ . The  $^1\text{H}$  NMR solution-state data are given in table 3.

Table 2. Selected mid-FTIR frequencies,  $\nu(\text{cm}^{-1})$  for tetra-kis(thione)Pt(II) complexes (**1**–**7**).

Compound	$\nu_{(\text{N-H})}$ ( $\text{cm}^{-1}$ )	$\nu_{(\text{C-S})}$ ( $\text{cm}^{-1}$ )
MeImt	3200 m	515 s
<b>1</b>	3172 m	503 s
EtImt	3188.2	514
<b>2</b>	3426 s	497
PrImt	3205 m	514 s
<b>3</b>	3202 s	507 sh
<i>i</i> -PrImt	3208.2	494, 526
<b>4</b>	3202 s	507 sh
EtDiaz	3220 m	453 s, 509 sh
<b>5</b>	3249 b	443 m, 512 sh
Diap	3214 s	526
<b>6</b>	3186 b	514 sh
<b>7</b>	3209 s	489, 520 sh

Note: m = medium, b = broad, s = strong, sh = shoulder.

Table 3.  $^1\text{H}$  chemical shifts (ppm) and couplings  $^3J_{\text{H-H}}$  (Hz) of the thiones and their tetrakis(thione)Pt(II) complexes (1–7) in  $\text{CDCl}_3$ .

Species	N–H	H–4 or H–5	H–6	N–C1–H	N–C2–H
MeImt <sup>a</sup>	7.95	3.58	3.36	2.93	
	s	t(8.85)	t(8.85)	s	
<b>1</b> <sup>a</sup>	9.41	3.78	3.58	3.00	
	s	t(8.90)	t(9.30)	s	
EtImt <sup>b</sup>	5.67	3.70	3.58	3.67	1.20
	s	m	t(8.70)	m	t(7.00)
<b>2</b>	9.67	3.71	3.56	3.67	1.19
	s	m	m	m	t(6.10)
PrImt <sup>b</sup>	5.88	3.71	3.58	3.56	1.64, 0.96 <sup>d</sup>
	s	t(8.70)	m	m	m(7.31), t(7.18)
<b>3</b>	9.58	3.73	3.58	3.46	1.63, 0.95 <sup>d</sup>
	s	t(8.93)	t(9.40)	t(7.48)	m(7.42), t(7.48)
<i>i</i> -PrImt <sup>b</sup>	5.63	3.61	3.57	4.82	1.19
	s	t(7.05)	t(7.30)	m	d(6.70)
<b>4</b>	9.65	3.82	3.73	4.45	1.20
	s	br s	t(8.25)	m	d(6.10)
EtDiaz <sup>b</sup>	6.31	3.34	2.01	3.28	3.91
	s	t(5.35)	m(5.15)	br s	m(6.82)
<b>5</b>	9.39	3.47	2.00	3.43	3.76
	s	br s	br s	br s	br s
Diap <sup>b</sup>	6.69	3.26	1.75	1.75	
	s	br s	br s	br s	
<b>6</b> <sup>c</sup>	9.09	3.30	1.71	1.71	
	s	br s	br s	br s	
<b>7</b> <sup>a</sup>	8.77	3.68	3.57	4.30	1.06

Note: s = singlet, d = doublet, t = triplet, m = multiplet, br = broad signal.

<sup>a</sup> $^1\text{H}$  resonances in DMSO.

<sup>b</sup> $^1\text{H}$  resonances of these thiones in DMSO are reported in literature [15, 16, 42].

<sup>c</sup> $^1\text{H}$  resonances of these complexes in 50 : 50 (v/v) mixture of  $\text{CDCl}_3$  and DMSO.

<sup>d</sup>N–C3–H.

The N–H protons of the coordinated thiones shift to higher frequency with respect to the free thiones. This de-shielding of the N–H protons is an indication of relatively more double bond character of the C–N bond upon coordination with Pt(II) center, consistent with the coordination of thiourea or its derivatives [30, 33–35]. The appearance of an N–H signal is a sign of coordinating with Pt(II) via the thione group.

H-4 of coordinated thiones is slightly downfield shifted in comparison to the free thiones due to double-bond character of the C–N bond upon coordination with Pt(II) through sulfur of the thiocarbonyl in thione ligands. There is no general trend observed in chemical shifts of H-5 and H-6, owing to different alkyl (methyl, ethyl, *n*-propyl and *iso*-propyl) groups attached to nitrogen of Imt containing ligands and different ring strains in R-Imt, EtDiaz, and Diap.

The  $^{13}\text{C}$  NMR solution-state data are given in table 4.  $^{13}\text{C}$  NMR signal for the thiocarbonyl carbon in all the complexes shifted upfield by 8–11 ppm with respect to the free ligands. This shift in thiocarbonyl carbon and NH proton signals is attributed to decrease in C=S bond order and increase in C–N bond order upon complexation [30, 34].

The solid-state  $^{13}\text{C}$  NMR, data shown in table 5, indicate that complexation of Pt(II) with the thiones resulted in shielding of thiocarbonyl carbons in the synthesized complexes by 8–10 ppm in comparison with their free thiones [36]. This also confirms that the ring form of thione is retained in the complexes. The *diap* ligand and the corresponding complex (**6**)



Table 4.  $^{13}\text{C}$  chemical shifts (ppm) of the thiones and their tetrakis(thione)Pt(II) complexes (1–7) in  $\text{CDCl}_3$ .

Species	C–2	C–4	C–5	C–6	N–C1	N–C2
MeImt <sup>a</sup>	182.90	40.60	50.18		33.39	
<b>1</b> <sup>a</sup>	173.55	42.27	51.68		33.60	
EtImt <sup>b</sup>	183.02	41.56	47.85		41.23	12.02
<b>2</b>	174.41	42.78	49.11		41.78	12.44
PrImt <sup>b</sup>	183.72	41.38	48.63		48.63	20.44, 11.18 <sup>d</sup>
<b>3</b>	174.90	42.80	49.66		48.48	20.60, 11.09 <sup>d</sup>
<i>i</i> -PrImt <sup>b</sup>	182.51	41.48	42.85		46.90	19.32
<b>4</b>	173.89	42.73	44.00		47.59	19.68
EtDiaz <sup>b</sup>	176.88	45.41	21.00	40.73	48.92	11.99
<b>5</b>	168.55	46.90	20.56	40.38	49.08	12.76
Diap <sup>b</sup>	189.42	46.28	27.33	27.33		
<b>6</b> <sup>c</sup>	178.27	46.25	26.43	26.43		
<b>7</b>	174.17	42.71	44.65		48.78	19.20

<sup>a</sup> $^{13}\text{C}$  resonances in DMSO.<sup>b</sup> $^{13}\text{C}$  resonances of these thiones in DMSO are reported in literature [15, 16, 42].<sup>c</sup> $^{13}\text{C}$  resonances of these complexes in 50 : 50 (v/v) mixture of  $\text{CDCl}_3$  and DMSO.<sup>d</sup>N–C3.Table 5. Solid-state  $^{15}\text{N}$  and  $^{13}\text{C}$  NMR chemical shifts (ppm) for free thione ligands and their tetrakis(thione)Pt(II) complexes (**1**, **5**, and **6**).

Species	N–1	C–2	C–4	C–5	C–6	N–C1	N–C2
MeImt	–275.29 – 277.41 <sup>a</sup>	180.97	40.68	50.85			34.19
<b>1</b>	–269.03 – 279.95 <sup>a</sup>	173.03	43.32	52.50			35.07 32.90 <sup>b</sup>
EtDiaz	–271.38 – 74.85 <sup>a</sup>	175.76	41.62	21.58	46.68	46.68	12.77
<b>5</b>	–258.24 – 270.75 <sup>a</sup>	168.82	41.58	20.69	48.40	48.40	12.73
		166.60					
Diap	–265.55	188.22	48.62	27.80	27.80		
		186.17	45.75				
		183.08	44.50				
<b>6</b>	–259.12 – 263.62 <sup>a</sup>	181.70	48.47	28.38	28.38		
		180.16	45.81	23.97	23.97		
		174.79	43.35				

<sup>a</sup>Resonance due to non-equivalent amino (–NH<sub>2</sub>) groups.<sup>b</sup>Resonance due to non-equivalent methyl (–CH<sub>3</sub>) groups.

showed three peaks in the thiocarbonyl region, attributed to different conformations of the seven-membered ring. According to the solid-state  $^{15}\text{N}$  spectra (table 5), the nitrogens in the synthesized complexes are 5–8 ppm de-shielded in comparison with their free ligands, confirming the increase in C–N bond order upon complexation.

### 3.3. Crystal structure determination of **1** and **7**

The X-ray structure of **1** is shown in figure 1 and the molecular packing in figure 1S (Supplementary material). The platinum(II) is located on an inversion center and bound to sulfurs of four N-methylimidazolidine-2-thione (MeImt) ligands in a distorted square planar geometry. The Pt–S bond distances are 2.3243(9) and 2.3263(9) Å and the S–Pt–S bond angle is 92.11(3)°. These values are in agreement with those reported for the complexes tetrakis(imidazolidine-2-thione)platinum(II) iodide [37] and tetrakis(thiourea-S)platinum(II) chloride [38]. The SCN<sub>2</sub> moieties of the two ligand molecules are essentially planar with the bond lengths (d(S1–C1) = 1.705(4) Å, d(C1–N1) = 1.321(5) Å, d(C1–N2) = 1.468(5) Å),

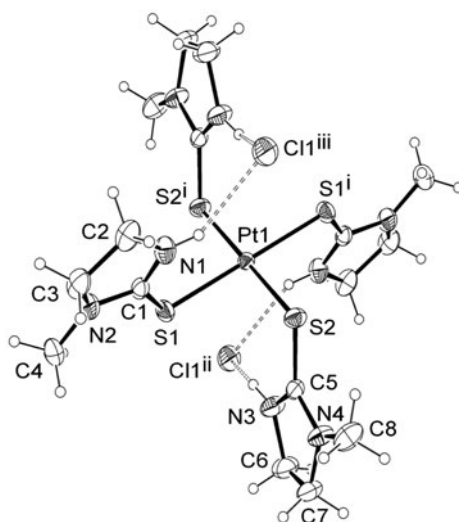


Figure 1. ORTEP diagram of **1** showing the atomic labeling scheme. Displacement ellipsoids are drawn at the 30% probability level. The hydration water was omitted for clarity. (Pt1–S1, 2.3243(9) Å; Pt1–S2, 2.3263(9) Å; S1–Pt1–S2, 92.11(3)°; S1–Pt1–S2<sup>i</sup>, 87.89(3)°). Symmetry codes: (i)  $-x, -y, -z$ ; (ii)  $-1-x, -1-y, -z$ ; (iii)  $1+x, 1+y, z$ .

and  $d(\text{S2}-\text{C5}) = 1.709(3)$  Å,  $d(\text{C5}-\text{N3}) = 1.313(5)$  Å,  $d(\text{C5}-\text{N4}) = 1.333(4)$  Å). The N–H groups (N1–H1 and N3–H3) of two *cis* thione ligands are engaged in hydrogen bonding with a common chloride giving a hydrogen bonding bridge  $[\text{N}-\text{H}\cdots\text{Cl}\cdots\text{H}-\text{N}]$  as shown in figure 1.

The X-ray structure of **7** is shown in figure 2 and the molecular packing in figure 2S (Supplementary material). Similar to **1**, Pt(II) is bonded to four sulfurs, each belonging to an N-isopropylimidazolidine-2-thione (*iPrImt*) ligand. The Pt–S bond lengths are 2.3035(8)–2.3222(8) Å while the S–Pt–S bond angles are 89.34(4)°–92.17(4)°. The bond distances are similar to those found for **1** and the related compound tetrakis(1-methyl-4-imidazoline-2-thione)platinum(II) chloride dihydrate [39]. Similar to **1**, the  $\text{SCN}_2$  moieties of the four ligand molecules are also essentially planar with the S–C and C–N bond lengths of 1.706(4)–1.709(4) Å and 1.321(4)–1.350(4) Å, respectively. However, the geometry around platinum exhibits interesting features. The structure presents a deviation from the ideal square planar geometry reminiscent of a bent see-saw distortion where the *trans*-sulfurs S1 and S1<sup>i</sup> are displaced above the  $[\text{PtS}_4]$  mean plane by 0.2603(9) Å whereas S2 and S2<sup>ii</sup> are displaced below the mean plane by 0.2723(8) Å. For **7**, the Pt coordination geometry can be more precisely described by the  $\tau_4$  (Tor4) parameter [40], as distorted square planar with a  $\tau_4$  value of 0.19 (the two largest angles in this four-coordinate species are 168.15(6)° and 165.38(5)°). In **1**, the Pt coordination geometry, which is located on an inversion center, has a perfect square planar geometry with  $\tau_4 = 0$  (the two largest angles in this four-coordinate species are both 180°). A closer look to hydrogen bonding interactions reveals that the thione ligands of each of the two *trans* pairs are engaged in hydrogen bonding interactions with one oxygen of the nitrate counter ion playing the role of a bridge between them:  $[\text{N}-\text{H}\cdots\text{O}_{\text{NO}_2}\cdots\text{H}-\text{N}]$ . This H-bonding scheme gives two decametallacycles

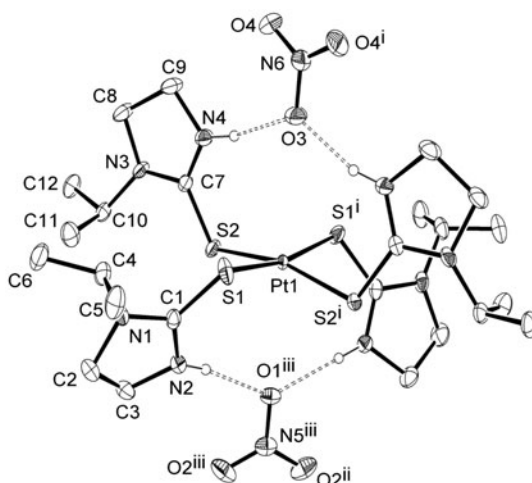


Figure 2. ORTEP diagram of **7** showing the atomic labeling scheme. Displacement ellipsoids are drawn at the 30% probability level. The hydration water and hydrogens other than N–H were omitted for clarity. (Pt1–S1, 2.3035(8) Å; Pt1–S2, 2.3222(8) Å; S1–Pt1–S2, 92.17(4)°; S1–Pt1–S2<sup>i</sup>, 89.34(4)°). Symmetry codes: (i)  $y, x, -z$ ; (ii)  $-y + 1/2, x - 1/2, z - 1/4$ ; (iii)  $x - 1/2, -y + 1/2, -z + 1/4$ .

[PtSCNH $\cdots$ O $\cdots$ HNCS] in which the *trans*-sulfurs are pushed out of the [PtS<sub>4</sub>] mean plane (figure 3) and hence resulting in the minor see-saw distortion. Hydrogen-bond geometry (Å, °) values of **7** are given in table 2S (Supplementary material).

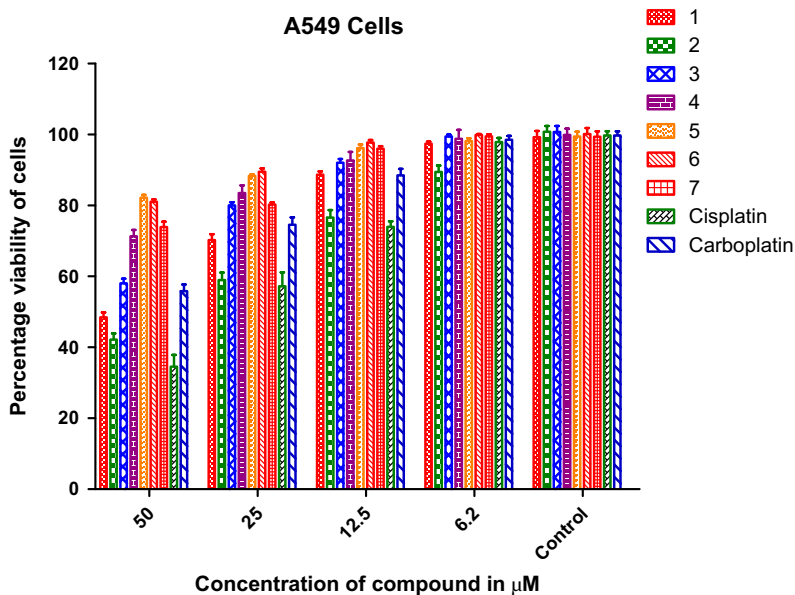


Figure 3. Effect of concentration of **1–7**, cisplatin and carboplatin in μM on the percentage viability of A549 cancer cells.

### 3.4. *In vitro* cytotoxicity of $[Pt(\text{thione})_4]Cl_2$ compounds against a panel of human cancer cell lines

The cytotoxicity of 1–7, cisplatin and carboplatin were evaluated *in vitro* against four human cancers, A549 (human lung carcinoma), MCF7 (human breast cancer), HCT15 (human colon adenocarcinoma), and HeLa (human cervical cancer) cell lines. The exposure of the cells to increasing concentrations of the complexes resulted in a dose-dependent cytotoxic effect. This cytotoxic effect was obtained by the stipulated increase in the concentrations of the complexes and cisplatin against a fixed number of human cancer cells. The  $IC_{50}$  concentration of the complexes, cisplatin and carboplatin for different human cell lines was obtained from curves between the complex concentration and percentage viability of the cells. Moreover, the effect of concentration of 1–7 in  $\mu\text{M}$  on the percentage viability of A549, MCF7, HCT15, and HeLa cells has been shown graphically in figures 3–6, respectively. The standard anticancer agents cisplatin and carboplatin were also included in the bar graphs (figures 3–6) for comparison with 1–7.

The  $IC_{50}$  values of the complexes ranged between 36.93 and 137.16  $\mu\text{M}$  for A549 cell line as given in table 6. Complex 2 has *in vitro* cytotoxicity comparable to that of cisplatin and almost two times better than that of carboplatin. Complexes 1 and 3 have *in vitro* cytotoxicity between cisplatin and carboplatin. Complexes 4 and 7 have almost equal cytotoxicity. The  $IC_{50}$  values of the complexes ranged between 11.40 and 120.86  $\mu\text{M}$  for MCF7 cell line as given in table 6. Complex 2 was two-fold better cytotoxic agent against the MCF7 cell line than cisplatin with  $IC_{50}$  values 11.40 and 21.33  $\mu\text{M}$ , respectively. Complexes 1, 4, and 7 have almost the same cytotoxicities. The  $IC_{50}$  values of the complexes ranged from 26.63 to 158.88  $\mu\text{M}$  for HCT15 cell line as given in table 6. Complex 2 has *in vitro* cytotoxicity between cisplatin and carboplatin. The  $IC_{50}$  values of the

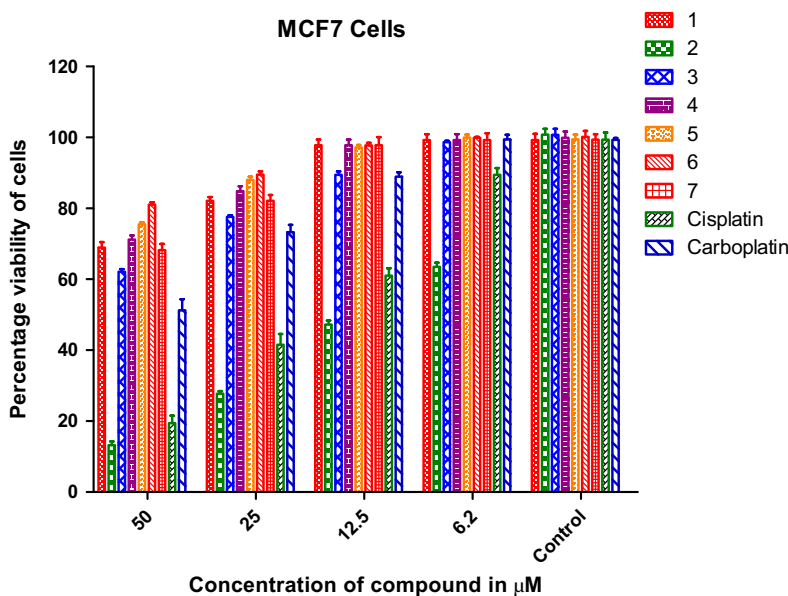


Figure 4. Effect of concentration of 1–7, cisplatin and carboplatin in  $\mu\text{M}$  on the percentage viability of MCF7 cancer cells.

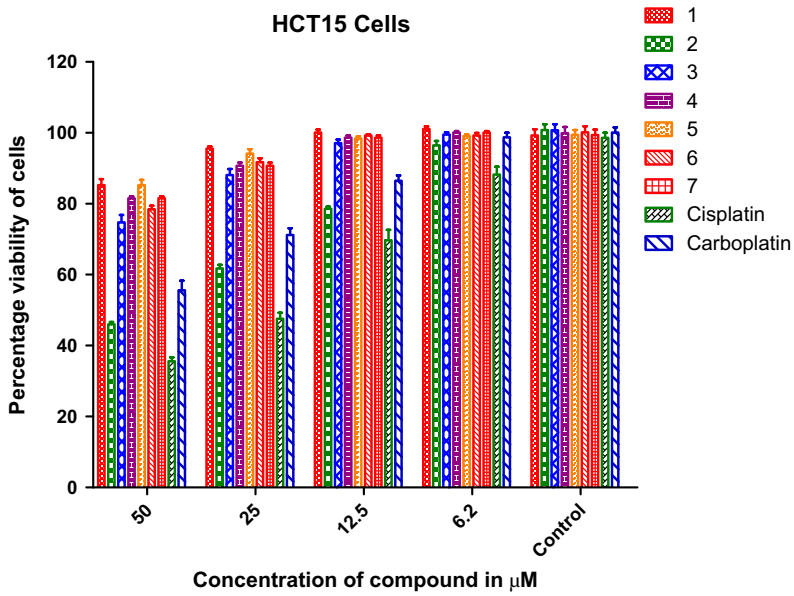


Figure 5. Effect of concentration of 1–7, cisplatin and carboplatin in  $\mu\text{M}$  on the percentage viability of HCT15 cancer cells.

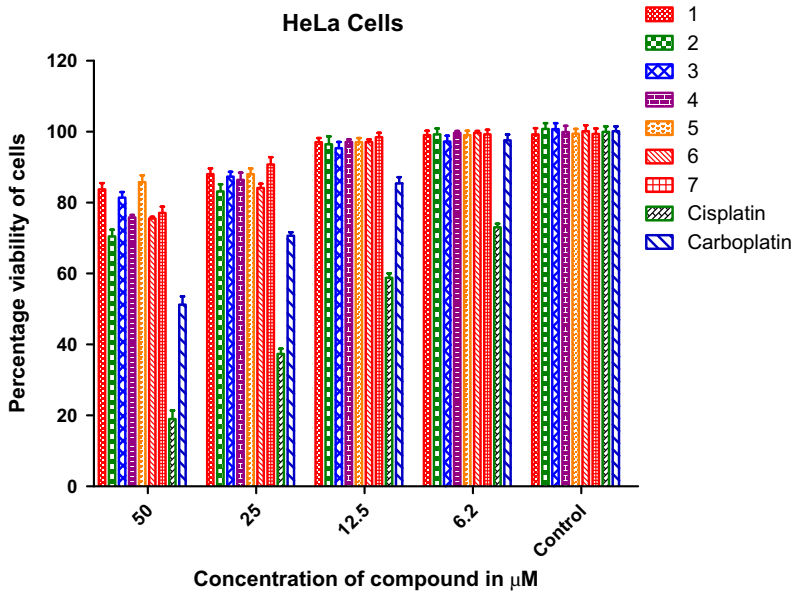


Figure 6. Effect of concentration of 1–7, cisplatin and carboplatin in  $\mu\text{M}$  on the percentage viability of HeLa cells.

Table 6. *In vitro* cytotoxic data of 1–7, cisplatin and carboplatin against A549, MCF7, HCT15, and HeLa cancer cell lines.

Compound	IC <sub>50</sub> ± SEM <sup>a</sup>			
	A549	MCF7	HCT15	HeLa
<b>1</b>	55 ± 1	75 ± 2	147 ± 2	142 ± 2
<b>2</b>	37 ± 1	11 ± 1	42 ± 2	79 ± 2
<b>3</b>	59 ± 3	63 ± 2	96 ± 2	133 ± 2
<b>4</b>	86 ± 1	78 ± 1	122 ± 2	95 ± 1
<b>5</b>	137 ± 2	95 ± 2	159 ± 3	166 ± 2
<b>6</b>	119 ± 2	121 ± 3	108 ± 2	92 ± 2
<b>7</b>	84 ± 1	74 ± 1	116 ± 2	100. ± 2
Cisplatin	37 ± 2	21 ± 2	27 ± 1	18 ± 1
Carboplatin	70 ± 2	53 ± 2	63 ± 2	55 ± 1

<sup>a</sup>Limit of errors is given in SEM as standard deviations determined from at least three independent experiments.

complexes 1–7 were 18.07–166.41 μM for HeLa cell line as given in table 6. Complexes 1–7 were not better than cisplatin and carboplatin.

The *in vitro* cytotoxicity of our complexes against HCT15 and HeLa cell lines was less than the parent drug cisplatin. These results are consistent with a significant selective cytotoxicity of 2 against particular cancer cell lines and its tendency to undergo ligand exchange with biomolecules like proteins and DNA [41–43].

#### 4. Conclusion

A series of complexes, [Pt(thione)<sub>4</sub>]X<sub>2</sub> (X<sup>-</sup> = Cl<sup>-</sup>, NO<sub>3</sub><sup>-</sup>), were synthesized and fully characterized using analytical techniques and spectroscopic methods. NMR as well as X-ray crystallography data confirmed that Pt(II) center is bonded to the thione ligands through sulfur. Hydrogen bonding interactions in 7 induce a bent see-saw distortion relative to ideal square planar geometry. *In vitro* cytotoxicity studies showed that [Pt(EtImt)<sub>4</sub>]Cl<sub>2</sub> (2) is the most effective and two-fold better cytotoxic agent than cisplatin against MCF7 (human breast cancer) cell.

#### Disclosure statement

No potential conflict of interest was reported by the authors.

#### Funding

This work was financially supported by the King Fahd University of Petroleum & Minerals (KFUPM) for the work through project No. [IN131018].

#### Supplemental data

Supplemental data for this article can be accessed here <http://dx.doi.10.1080/00958972.2015.1072175>.

## References

- [1] B. Rosenberg, L. Van Camp, T. Krigas. *Nature*, **205**, 698 (1965).
- [2] M. Goren, R. Wright, M. Horowitz. *Cancer Chemother. Pharmacol.*, **18**, 69 (1986).
- [3] L.R. Kelland, G. Abel, M.J. McKeage, M. Jones, P.M. Goddard, M. Valenti, B.A. Murrer, K.R. Harrap. *Cancer Res.*, **53**, 2581 (1993).
- [4] X. Wang, Z. Guo. *Chem. Soc. Rev.*, **42**, 202 (2013).
- [5] N. Muhammad, Z. Guo. *Curr. Opin. Chem. Biol.*, **19**, 144 (2014).
- [6] J.S. Butler, P.J. Sadler. *Curr. Opin. Chem. Biol.*, **17**, 175 (2013).
- [7] A. Muscella, N. Calabriso, S.A. De Pascali, L. Urso, A. Ciccacese, F.P. Fanizzi, D. Migoni, S. Marsigliante. *Biochem. Pharmacol.*, **74**, 28 (2007).
- [8] W. Friebolin, G. Schilling, M. Zöllner, E. Amtmann. *J. Med. Chem.*, **47**, 2256 (2004).
- [9] A.A. Ali, H. Nimir, C. Aktas, V. Huch, U. Rauch, K.-H. Schäfer, M. Veith. *Organometallics*, **31**, 2256 (2012).
- [10] R. del Campo, J.J. Criado, E. Garcia, M.R. Hermosa, A. Jiménez-Sánchez, J.L. Manzano, E. Monte, E. Rodríguez-Fernández, F. Sanz. *J. Inorg. Biochem.*, **89**, 74 (2002).
- [11] J. Ren, J. Diprose, J. Warren, R.M. Esnouf, L.E. Bird, S. Ikemizu, M. Slater, J. Milton, J. Balzarini, D.I. Stuart, D.K. Stammers. *J. Biol. Chem.*, **275**, 5633 (2000).
- [12] Z. Ma, L. Rao, U. Bierbach. *J. Med. Chem.*, **52**, 3424 (2009).
- [13] J.M. Brow, C.R. Pleatman, U. Bierbach. *Bioorg. Med. Chem. Lett.*, **12**, 2953 (2002).
- [14] A.Z.A. Mustafa, M. Altaf, M. Monim-ul-Mehboob, M. Fettouhi, M.I.M. Wazeer, A.A. Isab, V. Dhuna, G. Bhatia, K. Dhuna. *Inorg. Chem. Commun.*, **44**, 159 (2014).
- [15] G.D. Thorn. *Can. J. Chem.*, **33**, 1278 (1955).
- [16] L. Maier. *Helv. Chim. Acta*, **53**, 1417 (1970).
- [17] *SMART APEX software (5.05) for SMART APEX Detector*, Bruker Axs Inc., Madison, WI.
- [18] *SAINT Software (5.0) for SMART APEX Detector*, Bruker Axs Inc., Madison, WI.
- [19] G.M. Sheldrick. *SADABS. Program for Empirical Absorption Correction of Area Detector Data*, University of Gottingen, Göttingen, Germany (1996).
- [20] G.M. Sheldrick. *SHELXTL V5.1 Software*, Bruker Axs Inc., Madison, WI (1997).
- [21] G.M. Sheldrick. *Acta Crystallogr.*, **A64**, 112 (2008).
- [22] L. Farrugia. *J. Appl. Crystallogr.*, **30**, 565 (1997).
- [23] C.F. Macrae, I.J. Bruno, J.A. Chisholm, P.R. Edgington, P. McCabe, E. Pidcock, L. Rodriguez-Monge, R. Taylor, J. van de Streek, P.A. Wood. *J. Appl. Crystallogr.*, **41**, 466 (2008).
- [24] Stoe & Cie. *X-AREA & X-RED32*, Stoe & Cie GmbH, Darmstadt (2009).
- [25] A.L. Spek. *Acta Cryst.*, **D65**, 148 (2009).
- [26] M. Altaf, M. Monim-ul-Mehboob, A.A. Isab, V. Dhuna, G. Bhatia, K. Dhuna, S. Altuwajiri. *New J. Chem.*, **39**, 377 (2015).
- [27] J. Jolley, W.I. Cross, R.G. Pritchard, C.A. McAuliffe, K.B. Nolan. *Inorg. Chim. Acta*, **315**, 36 (2001).
- [28] J. Lin, G. Lu, L.M. Daniels, X. Wei, J.B. Sapp, Y. Deng. *J. Coord. Chem.*, **61**, 2457 (2008).
- [29] M. Altaf, H. Stoeckli-Evans, A. Cuin, D.N. Sato, F.R. Pavan, C.Q.F. Leite, S. Ahmad, M. Bouakka, M. Mimouni, F.Z. Khardli, T.B. Hadda. *Polyhedron*, **62**, 138 (2013).
- [30] P. Castan, J. Laurent. *Transition Met. Chem.*, **5**, 154 (1980).
- [31] B.H. Abdullah, M.A. Abdullah, S.A. Al-Jibori. *Asian J. Chem.*, **19**, 1334 (2007).
- [32] A.-M. Esmadi. *Asian J. Chem.*, **13**, 128 (2001).
- [33] S. Schröder, W. Preetz. *Z. Anorg. Allg. Chem.*, **626**, 1757 (2000).
- [34] A.A. Isab, M.I.M. Wazeer. *J. Coord. Chem.*, **58**, 529 (2005).
- [35] A.A. Isab, S. Ahmad, M. Arab. *Polyhedron*, **21**, 1267 (2002).
- [36] M.I.M. Wazeer, A.A. Isab, A. El-Rayyes. *Spectroscopy*, **18**, 113 (2004).
- [37] J. Lin, G. Lu, L. Daniels, X. Wei, J. Sapp, Y. Deng. *J. Coord. Chem.*, **61**, 2457 (2008).
- [38] L. Fuks, N. Sadlej-Sosnowska, K. Samochocka, W. Starosta. *J. Mol. Struct.*, **740**, 229 (2005).
- [39] P.J.M.W.L. Birker, J. Reedijk, G.C. Verschoor, J. Jordanov. *Acta Crystallogr., Sect. B*, **38**, 2245 (1982).
- [40] L. Yang, D.R. Powell, R.P. Houser. *Dalton Trans.*, 955 (2007).
- [41] S.U. Rehman, A.A. Isab, M.N. Tahir, T. Khalid, M. Saleem, H. Sadaf, S. Ahmad. *Inorg. Chem. Commun.*, **36**, 68 (2013).
- [42] D. Kovala-Demertzi, M.A. Demertzis, J.R. Miller, C. Papadopoulou, C. Dodorou, G. Filousis. *J. Inorg. Biochem.*, **86**, 555 (2001).
- [43] S. Ahmad, A.A. Isab, S. Ali, A.R. Al-Arfaj. *Polyhedron*, **25**, 1631 (2006).